COMPOSITES SCIENCE AND TECHNOLOGY

Volume 103, 28 October 2014, Pages 106–112

DOI: 10.1016/j.compscitech.2014.08.018

http://www.sciencedirect.com/science/article/pii/S0266353814002991

WOOD FIBER REINFORCED MULTICOMPONENT, MULTIPHASE PP COMPOSITES: STRUCTURE, PROPERTIES, FAILURE MECHANISM

András Sudár[1,2], Christoph Burgstaller[3], Károly Renner[1,2,*], János Móczó[1,2] and Béla Pukánszky[1,2]

[1]Laboratory of Plastics and Rubber Technology, Department of Physical Chemistry and Materials Science, Budapest University of Technology and Economics, H-1521 Budapest, P.O. Box 91, Hungary

[2]Institute of Materials and Environmental Chemistry, Research Centre for Natural Sciences, Hungarian Academy of Sciences, H-1519 Budapest, P.O. Box 286, Hungary

[3]Transfercenter für Kunststofftechnik GmbH, Franz-Fritsch-Strasse 11, A-4600 Wels, Austria

*Corresponding author: Phone: +36-1-463-2479, Fax: +36-1-463-3474, E-mail: krenner@mail.bme.hu

KEYWORDS: A: Polymer-matrix composites (PMCs), A: Recycling, B: Interfacial strength, C: Damage mechanics, Bumper material

ABSTRACT

Polypropylene (PP) was reinforced with wood flour and impact modified with elastomers to increase stiffness and impact resistance simultaneously. Elastomer was added in 0, 5, 10 and 20 wt%, while wood content changed from 0 to 60 wt% in 10 wt% steps. Structure and adhesion were controlled by the addition of functionalized (maleated) polymers. Composites were homogenized in a twin-screw extruder and then injection molded to tensile bars. The results showed that composite structure is determined by the relative strength of adhesion and shear forces prevailing during processing. Structure can be controlled by the application of functional polymers within limits. Although embedding is favored by thermodynamics and further promoted by coupling, de-encapsulation occurs at the large shear stresses of injection molding even in the presence of a functionalized elastomer. Composite properties depend on composition, increasing elastomer content results in decreasing stiffness and strength. Model calculations showed that the elastomer does not contribute to load bearing, average stress in the matrix increases with increasing elastomer content. Local stresses and adhesion define the initiation of deformation processes around wood particles, which start at the same stress irrespectively of elastomer content. Local processes determine the mechanism of failure and composite strength independently of their mechanism.

1. INTRODUCTION

Wood flour and natural fibers are used in increasing quantities for the reinforcement of commodity, but recently also for other thermoplastic polymers [1-5]. Such reinforcements have many advantages over particulate fillers or glass fibers; they increase stiffness considerably, are obtained from renewable resources, available in abundant quantities, cheap, and light at the same time [2,6,7]. Major application areas of these materials are the building and the automotive industries. Cars contain a considerable amount of plastics; one of the main plastic parts is the bumper. Current laws require the recycling of all components of cars, thus they are shredded after their useful life producing a large amount of plastic waste. Such waste can be upgraded with the incorporation of natural fibers resulting in materials, which can be used, among others,

for the preparation of car parts again. Several attempts have been reported recently for the production of composites prepared from plastic waste and natural fibers [8-10].

In structural applications often large stiffness and impact resistance are required simultaneously, which are achieved by the combination of several functional additives, e.g. an elastomer to improve impact resistance and a mineral filler or glass fiber to increase stiffness [11-13]. Research has started as early as the 80ies on these materials [11,14-17] and they are commercially available for several decades. Two boundary structures may form in such multicomponent materials: the two components, i.e. the elastomer and the filler, can be distributed separately from each other in the polymer matrix [18-20], or the elastomer may encapsulate the reinforcement to create embedded structure [11-13,21]. The actual structure is determined by the adhesion and shear forces prevailing in the melt during homogenization, the first favors embedding because of thermodynamic reasons, while the second promotes separate dispersion through the shearing of the elastomer layer apart from the filler [22]. Usually intermediate structures form in composites produced under practical conditions, a part of the filler is embedded into the elastomer phase, but individual elastomer droplets and filler particles can be also located in the matrix. Structure can be tailored by the control of interfacial adhesion through the use of appropriate coupling agents [23-26]. Functionalized polymers are used to control structure in polypropylene. The introduction of maleated PP (MAPP) leads almost exclusively to the separate dispersion of the components [27-29]. Adhesion force changes from about 100 mJ/m^2 to nearly 1000 mJ/m^2 in this way [30]. The addition of maleated ethylene-propylene-diene elastomer (MAEPDM), on the other hand, results in a large extent of embedding. Properties change considerably with structure even at the same composition. Stiffness was shown to depend mainly on the extent of embedding, while impact resistance was influenced also by other factors including micromechanical deformation processes occurring around the inclusions (elastomer, filler) [31].

The incorporation of wood and/or natural fibers into such composites may modify structure and properties considerably. Wood particles are large, usually several 100 μm in size that facilitates debonding, the separation of the matrix/filler interface already at small stresses [32,33]. A functionalized polymer coupling agent is needed practically always in order to

achieve reasonable properties in PP. Besides debonding, large wood particles may initiate other micromechanical deformation processes during deformation like fiber pull-out, or fiber fracture occurring at strong interfacial adhesion [33,34]. These differences compared to particulate fillers and the tendency to replace traditional reinforcements with natural ones require the more detailed study of the behavior of multicomponent materials containing wood fibers, since information is rather scarce on these materials yet. A model study was carried out on the recycling of PP/PE blends by Clemons [35], and functionalized elastomers were used to modify structure and properties in PP/wood composites by Oksman [36,37]. The goal of our study was to model recycled bumper materials by combining polypropylene, wood flour and an elastomer. Structure was controlled by the use of functionalized polymers. We intended to identify the factors determining the structure and properties of such materials and to analyze deformation and failure processes in detail. The practical relevance of these latter is discussed briefly in the final section of the paper.

2. EXPERIMENTAL

The polymer used in the study was the Tipplen H 781 F grade PP homopolymer (MFR = 0.7 g/10 min at 230 °C and 2.16 kg load) produced by TVK, Hungary. The Vistalon 706 ethylene-propylene-diene (EPR) elastomer (ethylene content: 65 wt%, Mooney viscosity ML1+4 at 125 °C: 42) of Exxon Mobil, USA was used to increase impact resistance. The functionalized polymers applied for the control of structure and interfacial adhesion were the Orevac CA 100 grade maleated PP (MFR = 150-200 g/10 min at 230 °C and 2.16 kg, MA content: 1.0 wt%) from Arkema, France and the Exxcellor VA 1803 maleated EPDM (ethylene content: 43 wt%, MFR = 3 g/10 min at 230 °C and 2.16 kg, MA content: 0.5-1.0 wt%) from Exxon Mobil, USA. The Filtracel EFC 1000 wood flour was supplied by Rettenmaier and Söhne GmbH, Germany. The wood was treated to remove waxes by the producer, it contained 70.4 wt% holocellulose, 28.7 wt% lignin and 0.9 wt% waxes. The filler had an average particle size of 210 μm as determined by laser light scattering. Scanning electron microscopy (SEM) analysis of particle geometry showed an average particle length of 363 μm, diameter of 64 μm and aspect ratio of 6.8. MAPP was always added in 10 wt% calculated for the amount of wood [38], while the

impact modifiers (EPR, MAEPDM) were introduced in 5, 10 and 20 wt% of the matrix polymer. Wood content changed from 0 to 60 wt% in 10 wt% steps related to the total weight of the composites.

The composites were homogenized using a ThermoPrism TSE 24 (Thermo Fisher Sci. Inc., USA) twin-screw extruder with a screw diameter of 24 mm and an L/D ratio of 28. Screw configuration included two kneading zones with different lengths and conveying elements. The polymer components were introduced into the hopper, while wood was added to the melt through a side feeder. Zone temperatures were set from 170 to 220 °C in 10 °C steps in the six zones of the extruder. The granulated material was dried for 4 hours at 105 °C in an oven and then injection molded to standard ISO 527 1A tensile specimens using a Demag IntElect 50 machine (Demag Ergotech GmbH, Germany) at 170-180-190-200-210 °C zone and 50 °C mold temperatures, 50 mm/s injection rate, 1300 bar holding pressure and 25 sec holding time. The samples were conditioned at 23 °C and 50 % RH for a week before testing. For selected compositions granules were also homogenized in a Brabender W 50 EHT internal mixer (190 °C, 50 rpm for 10 min) in order to demonstrate the effect of processing conditions on composite properties. The homogenized material was compression molded into 1 mm thick plates at 190 °C using a Fontijne SRA 100 machine.

Tensile testing was carried out with an Instron 5566 type machine (Instron Co., USA). Stiffness was determined at 0.5 mm/min, while other tensile characteristics like yield stress, yield strain, tensile strength and elongation-at-break at 5 mm/min cross-head speed and 115 mm gauge length. The structure of the composites was studied by scanning electron microscopy using a Jeol JSM 6380 LA apparatus (JEOL Ltd., Tokyo, Japan). The distribution of the components in the matrix was determined on fracture surfaces created at liquid nitrogen temperature. Samples containing an elastomer component were etched in n-hexane for 1 min. SEM micrographs were recorded also on fracture surfaces created in the tensile test in order to determine the mechanism of failure. Etching was used when appropriate.

3. RESULTS AND DISCUSSION

The combination of all the compositional variables resulted in a very large number of

composites. As a consequence we refrain from the presentation of all results and focus our attention on selected materials. On the other hand, all the results are presented in figures showing general correlations. In the first two sections we describe structure and tensile properties, while deformation and failure mechanism is analyzed in detail in the next part of the paper. General correlations and practical consequences are discussed in the last section.

3.1. Structure

Several structure related phenomena may influence the properties of multi-component PP composites. The major issue is the dispersion of the components, the formation of dispersed or embedded structures. Wood particles with anisotropic particle geometry orientate during injection molding and the fibers may also associate at large wood contents [38]. The composition dependence of modulus offers information about the first issue, i.e. dispersion, but also on the possible aggregation of the particles. Since all specimens were prepared with the same technology under the same conditions, we assume that orientation is the same or very similar in all of them, thus this issue is not considered and discussed in detail in the further parts of the paper.

The stiffness of PP/wood composites containing various amounts of functionalized ethylene-propylene-diene copolymer (MAEPDM) is plotted against wood content in **Fig. 1**. PP/wood and PP/MAPP/wood composites show the same composition dependence, the stiffness of the two is practically identical. The two composites differ only in interfacial adhesion and stress transfer and modulus is influenced only slightly by this factor. Stiffness increases significantly with increasing wood content as expected. Deviation from the general tendency can be observed only at very large wood content, probably because of the association of wood particles. Slightly changing orientation may also result in such deviations [1, 39]. The presence of the elastomer decreases modulus, and in the case of separate dispersion the stiffness vs. wood content correlations are expected to run parallel to that of PP/wood composites. If a part or all of the wood particles are embedded into the elastomer a correlation with smaller slope should describe the modulus vs. wood content correlation. As **Fig. 1** shows, the slope of the correlations is only slightly smaller at all three elastomer contents than that of the PP/wood composite, thus the extent of embedding is small, only a small part of the wood particles is located within

the elastomer phase. We drew only three lines in the figure to facilitate viewing. The lines indicate trends and they serve only to guide the eye in this and in all other figures. Deviation from the general trend does not show systematic variation indicating random changes in structure (embedding, dispersion, orientation).

The composition dependence of stiffness is compared for the five combinations of materials (PP, PP/MAPP, PP/EPR, PP/EPR/MAPP, PP/MAEPDM) in **Fig. 2** at 10 wt% elastomer content. We can see that four of the correlations run together, only the presence of MAEPDM results in a limited extent of encapsulation. Deviations from the general tendency occur only at larger wood contents. The results presented in **Fig. 1 and 2** prove that the elastomer decreases modulus irrespectively of its type (EPR or MAEPDM), as expected, MAEPDM promotes some embedding, and structure varies at large wood content for all combinations of materials because of changing dispersion and/or orientation. These conclusions are strongly corroborated by **Fig. 3** showing the SEM micrograph recorded on the cryo-fractured and etched surface of the composite containing 30 wt% wood and 20 wt% MAEPDM. According to the micrograph wood particles are firmly embedded into the PP matrix and the elastomer is dispersed mainly in the form of submicron particles separately from wood.

3.2. Properties

Wood flour increases the stiffness of PP and PP/elastomer blends. The extent of increase depends on wood and elastomer content and on structure, on the extent of embedding. These relationships are clearly shown by **Figs. 1 and 2**. Modulus does not depend much on interfacial adhesion, but properties measured at larger deformations do. The dependence of tensile yield stress on wood content is presented in **Fig. 4**. The correlations differ considerably from those shown in the previous section; the effect of interfacial adhesion is clear. The application of the maleated PP coupling agent results in a tenfold increase of interfacial adhesion [30] and results in strong reinforcement both in the absence and the presence of EPR. Without MAPP, tensile yield stress decreases with increasing wood content in PP/wood composites. The presence of the elastomer component results in a decrease in tensile yield stress as well. The effect is independent of the type of the elastomer used. The correlation is parallel to that obtained for the

PP/wood composite indicating that structure and interaction do not change much in the presence of either EPR or MAEPDM in accordance with the conclusions presented in the previous section. The composition dependence of tensile strength is very similar to that of yield stress with the complicating effect of changing specimen dimensions during deformation which covers a wide range from 2 to almost 1000 %, if we consider all the blends and composites studied. Deformation decreases drastically with increasing wood content (not shown) further complicating the evaluation of the composition dependence of tensile strength. The drastic difference in the composition dependence of yield stress at poor (without MAPP) or good (with MAPP) adhesion, respectively, also indicates changing deformation mechanism.

3.3. Deformation and failure mechanism

The studied composites are heterogeneous materials with the consequence of the development of a heterogeneous stress field around the inclusions due to the dissimilar elastic properties of the components. Usually stress concentration develops around particles dispersed in the matrix, either filler or elastomer, resulting in local deformation processes occurring around them. These local deformation processes were shown to determine the macroscopic properties of the composites [34,40]. Local processes can be studied by various means; acoustic emission and volume strain measurements are the two most often used techniques. In this study we followed local, micromechanical deformation processes by acoustic emission, which detects the emission of elastic waves upon a local burst like event around the particle with the help of a piezoelectric sensor.

The result of such a measurement is presented in **Fig. 5**. The steeply increasing curve on the left hand side of the plot is the stress vs. deformation correlation which is shown for reference. The small circles are individual acoustic events, hits or signals, detected during the deformation of the specimen. We can see that a very large number, almost 14000 events were detected in this PP composite containing 30 wt% wood. Signals start to appear above a certain deformation indicating that the local event has a threshold deformation or stress. The signals form two groups, a smaller one up to about 1.5-1.7 % deformation and a larger one for the

remaining part of the test. The average amplitude of the signals – their vertical position is proportional to their amplitude – also differs in the two groups. It is difficult to draw further conclusions from individual signals, thus the cumulative number of signals, i.e. the sum of all signals up to the given deformation, is also plotted in the figure. This clearly shows that two consecutive processes take place during deformation, the first appears as a small step, while the second as an increasing section of the correlation. The shape of the cumulative number of signal vs. deformation trace offers information about the micromechanical processes occurring [33,34] and characteristic stress values (σ_{AE}) can be also derived from the correlations which are related to the initiation of the individual processes.

In **Fig. 6** the cumulative number of signal vs. deformation traces are compared for five combinations of materials containing 30 wt% wood and 10 wt% elastomer. The corresponding stress vs. strain traces are also included as reference. Although the comparison of the traces is not easy, it indicates some difference among the materials. Good adhesion (MAPP) results in a large number of signals and a steep increase in the cumulative number of signal trace (PP/MAPP, PP/EPR/MAPP). The number of signals is smaller at poor adhesion (PP, PP/EPR) and two steps can be detected on the traces. Considerably less signals evolve in the PP/MAEPDM/wood composites caused mainly by dissimilar adhesion and embedding, since otherwise most properties were very similar for the PP/EPR and the PP/MEPDM composites (see **Figs. 2 and 4**).

Characteristic stresses determined for the PP/MAEPDM/wood composites are plotted as a function of wood content in **Fig. 7**. Two sets of correlations can be observed in the figure. The first consists of a single series, it belongs to the PP/MAPP composites and shows that the initiation stress for the dominating process increases with wood content. Such a correlation was assigned to the fracture of wood particles earlier [33]. Initiation stress is practically independent of wood content for the rest of the composites belonging to the second set and decreases with increasing elastomer content. The dominating local deformation process can be debonding or the pull-out of the fibers. Similar correlations were obtained for the PP/EPR composites as well (not shown). The primary values of characteristic stresses indicate that the elastomer facilitates the initiation of the dominating deformation process that is quite hard to believe, since we

showed that mainly separately distributed structure develops in these composites. Further considerations are needed to explain the phenomenon.

Considering that in the absence of MAPP adhesion is poor between the matrix and wood, on the one hand, and that the elastomer does not carry much load because of its small stiffness, we must come to the conclusion that local stresses around the wood particles change with increasing elastomer content. If we assume that the elastomer does not contribute to load-bearing, the average stress in the matrix can be calculated from the effective load-bearing cross section of the specimen. A correlation was proposed by Nicolais and Narkis [41], but the load-bearing cross-section calculated by their formula goes to zero at a definite filler volume fraction which is smaller than 1. Another correlation remedies this deficiency and gives the effective load-bearing cross-section (Ψ) in the form

$$\Psi = \frac{1-\varphi_e}{1+2.5\,\varphi_e} \qquad (1)$$

and the average stress in the matrix corrected by the effect of load-bearing cross-section in this way is

$$\sigma_{AE}^{corr} = \sigma_{AE}\frac{1+2.5\,\varphi_e}{1-\varphi_e} \qquad (2)$$

where σ_{AE} is the characteristic stress determined by acoustic emission and φ_e is the volume fraction of the elastomer in the composite. Corrected characteristic stress is plotted against wood content in **Fig. 8** for the same composites as in the previous figure (**Fig. 7**). We can see that all points fall onto the same correlation indicating that the dominating local process is initiated at the same stress, which implies that the elastomer is distributed separately from wood and it does not carry any load indeed. Corrected initiation stress is plotted for all material combinations in **Fig. 9** at 10 wt% elastomer content. We can see that the relationships shown for the PP/MAEPDM/wood composites are valid for all combination of materials. The presence of MAPP leads to a considerable increase of initiation stress, while a different local deformation occurs in materials with poor adhesion which is initiated at the same stress independently of elastomer or wood content. The empty symbols represent the first process (first step on the cumulative number of signal vs. deformation traces, see **Fig. 5**), which is also independent of elastomer and wood content, but occurs at a smaller stress, thus it must be different from the

second process.

The only question which remains is the identification of the processes occurring in the different material combinations. Although the shape of the cumulative signal traces and the composition dependence of the characteristic stress indicated that fiber fracture, pull-out or debonding may be the processes involved in the order of decreasing initiation stress, SEM micrographs might offer further support and proof for them. A few representative SEM micrographs are presented in **Fig 10**. The micrograph in **Fig. 10a** was recorded on a PP/MAPP wood composite containing 30 wt% wood. The fracture of several wood particles can be seen clearly in the photo. Debonding and pull-out are the dominating processes in the PP/EPR/wood composites (**Fig. 10b and 10c**), which change to fracture again in PP/EPR/MAPP/wood composites (**Fig. 10d**) confirming our analysis based on micromechanical testing (acoustic emission).

3.4. Discussion

Although the results are rather unambiguous and we could explain most questions related to structure, deformation and properties, a few issues merit additional considerations. By the analysis of the composition dependence of modulus we came to the conclusion that the extent of embedding is small in all composites, which is quite surprising, since MAEPDM was used in order to achieve excessive or even exclusive embedding. We know that the extent of embedding depends on the relative magnitude of adhesion and shear forces during mixing. Adhesion is determined by interfacial interactions, while shear depends on processing conditions. The effect of this latter factor is shown in **Fig. 11** in which we compare the stiffness, i.e. the extent of embedding, for compression and injection molded samples. The modulus of composites containing MAPP is also plotted as reference; such composites were shown to possess separately dispersed components. The modulus of these composites is independent of processing technology showing separate dispersion. The small stiffness of compression molded specimens prepared from composites containing MAEPDM proves that a large extent of embedding is achieved in this case indeed. On the other hand, the modulus of specimens prepared from the same composites by injection molding is considerably larger indicating that the large shear of this processing technology results in de-encapsulation, in the separate dispersion of the

components. These results clearly prove our conclusions drawn about the structure of the composites.

The second issue which needs further consideration is the relationship of local processes and the macroscopic properties of the composites. The tensile strength of all composites studied is plotted against the characteristic stress of the dominating deformation process detected by acoustic emission in **Fig. 12**. The initiation stress of the second process is plotted in the graph for composites in which two consecutive processes were detected. An extremely close correlation is obtained indicating that the local process determines the performance of the composite irrespectively of the mechanism of the deformation. The close relationship also means that the composite fails almost immediately after the initiation of the local deformation process mainly in or around the wood particles. Accordingly, these processes must be controlled in order to develop composites with improved properties, i.e. larger yield stress and tensile strength.

4. CONCLUSIONS

The study of five sets of PP composites reinforced with wood fibers and impact modified with an elastomer showed that composite structure is determined by the relative strength of adhesion and shear forces prevailing during processing. Structure can be controlled by the application of functional polymers within limits. Although embedding is favored by thermodynamics and further promoted by coupling, de-encapsulation occurs at the large shear stresses of injection molding even in the presence of a functionalized elastomer. Composite properties depend on composition, increasing elastomer content results in decreasing stiffness and strength. Model calculations showed that the elastomer does not contribute to load-bearing, average stress in the matrix increases with increasing elastomer content. Local stresses and adhesion define the initiation of deformation processes around wood particles, which start at the same stress irrespectively of elastomer content. Local processes determine the mechanism of failure and composite strength independently of their mechanism.

5. ACKNOWLEDGEMENTS

The authors are indebted to Zsolt László for his help in the determination of the particle characteristics of wood. The research on heterogeneous polymer systems was financed by the

National Scientific Research Fund of Hungary (OTKA Grant No. K 101124) and by the Forbioplast FP7 project of EC (212239); we appreciate the support very much. One of the authors (KR) is grateful also to the János Bolyai Research Scholarship of the Hungarian Academy of Sciences for its support.

6. REFERENCES

1. Bledzki AK, Sperber VE, Faruk O. Natural and wood fibre reinforcement in polymers. Rapra Vol. 13., Shawbury; 2002.
2. Bledzki AK, Gassan J. Composites reinforced with cellulose based fibres. Prog Polym Sci 1999;24:221–274.
3. Bledzki AK, Faruk O, Huque M. Physico-mechanical studies of wood fiber reinforced composites. Polym-Plast Technol 2002;41:435– 451.
4. Graupner N, Herrmanna AS, Müssig J. Natural and man-made cellulose fibre-reinforced poly(lactic acid) (PLA) composites: An overview about mechanical characteristics and application areas. Compos Part A 2009;40:810-821.
5. Peltolaa H, Pääkkönenb E, Jetsub P, Heinemann S. Wood based PLA and PP composites: Effect of fibre type and matrix polymer on fibre morphology, dispersion and composite properties. Compos Part A 2014;61:13-22.
6. Bledzki AK, Mamun AA, Volk J. Physical, chemical and surface properties of wheat husk, rye husk and soft wood and their polypropylene composites. Compos Part A 2010;41:480–488.
7. La Mantia FP, Morreale M. Green composites: A brief review. Compos Part A 2011;42: 579–588.
8. Pal K, Mukherjee M, Frackowiak S, Koylowski M, Das CK. Improvement of the physic-mechanical properties and stability of waste polypropylene in the presence of wood flour and (maleic andhydride)-grafted polypropylene. J Vinyl Addit Technol 2014;20:24-30.
9. Kazemi Y, Cloutier A, Rodrigue D. Mechanical and morphological properties of wood plastic composites based on municipal plastic waste. Polym Compos 2013;34:487-493.
10. Carvalho Neto AGV, Ganzerli TA, Cardozo AL, Favaro SL, Pereira AGB, Girotto EM, Radovanovic E. Development of composites based on recycled polyethylene/sugarcane bagasse fibers. Polym Compos 2014;35:768-774.
11. Stamhuis JE. Mechanical properties and morphology of polypropylene composites. Talc-filled, elastomer-modified polypropylene. Polym Compos 1984;5:202–207.
12. Stamhuis JE. Mechanical properties and morphology of polypropylene composites II. Effect of polar components in talc-filled polypropylene. Polym Compos 1988;9:72–77.
13. Stamhuis JE. Mechanical properties and morphology of polypropylene composites. III. Short glass fiber reinforced elastomer modified polypropylene. Polym Compos 1988;9:280–284.
14. Serafimow BL. Rheological properties of multicomponent mixtures based on polypropylene. Plaste Kautsch 1982;29:598–600.
15. Comitov PG, Nicolova ZG, Siméonov IS, Naide-Nova KV, Siarova AD. Basic polypropylene com- positions possessing an improved shock resistance (in French). Eur Polym J 1984;20:405–407.
16. Lee YD, Lu CC: The mechanical and rheological properties of EPR modified PP composites. J Chin Inst Chem Eng 1982;13:1–8.
17. Dao KC, Hatem RA. Properties of blends of rubber/talc/polypropylene in Proceedings of the SPE Antec 84. 1984;42:198–204.
18. Kolarík J, Lednický F. Structure of polypropylene/ EPDM elastomer/calcium carbonate composites in Polymer composites, (eds.: Sedlácek B.) Walter de Gruyter 1986;537–544.

19. Premphet K, Horanont P. Influence of stearic acid treatment of filler particles on the structure and properties of ternary-phase polypropylene composites. J Appl Polym Sci 1999;74:3445–3454.
20. Hornsby PR, Premphet K. Influence of phase microstructure on the mechanical properties of ternary phase polypropylene composites. J Appl Polym Sci 1998;70:587–597.
21. Pukánszky B, Kolarík J, Lednický F. Mechanical properties of three-component polypropylene composites in Polymer composites, (eds.: Sedlácek B.) Walter de Gruyter 1986;553–560.
22. Pukánszky B, Tüdős F, Kolarík J, Lednický F. Ternary composites of polypropylene, elastomer, and filler: Analysis of phase structure formation. Polym Composite 1990;11:98–104.
23. Kelnar I. The effect of PP and EPR grafted with acrylic acid on the properties and phase structure of polypropylene/elastomer/short glass fibre composites. Angew Makromol Chem 1991;189:207–218.
24. Chiang W-Y, Yang W-D. Polypropylene composites. I. Studies of the effect of grafting of acrylic acid and silane coupling agent on the performance of polypropylene mica composites. J Appl Polym Sci 1988;35:807–823.
25. Chiang WY, Yang WD, Pukánszky B. Polypropylene composites. II: Structure-property relationships in two- and three-component polypropylene composites. Polym Eng Sci 1992;32:641–648.
26. Kolarík J, Lednický F, Jancar J, Pukánszky B. Phase-structure of ternary composites consisting of polypropylene elastomer filler – Effect of functionalized components. Polym Commun 1990;31:201– 204.
27. Felix JM, Gatenholm P. The nature of adhesion in composites of modified cellulose fibers and polypropylene. J Appl Polym Sci 1991;42:609– 620.
28. Kazayawoko M, Balatinecz JJ, Woodhams RT. Diffuse reflectance Fourier transform infrared spectra of wood fibers treated with maleated polypropylenes. J Appl Polym Sci 1997;66:1163–1173.
29. Kazayawoko M, Balatinecz JJ, Matuana LM. Surface modification and adhesion mechanisms in wood-fiber-polypropylene composites. J Mater Sci 1999;34:6189–6199.
30. Renner K, Móczó J, Vörös G, Pukánszky B. Quantitative determination of interfacial adhesion in composites with strong bonding. Eur Polym J 2010;46:2000–2004.
31. Molnár Sz, Pukánszky B, Hammer CO, Maurer FHJ. Impact fracture study of multicomponent polypropylene composites. Polymer 2000;41:1529–1539.
32. Móczó J, Pukánszky B. Polymer micro and nanocomposites: Structure, interactions, properties. J Ind Eng Chem 2008;14:535–563.
33. Renner K, Móczó J, Pukánszky B. Deformation and failure of PP composites reinforced with lignocellulosic fibers: Effect of inherent strength of the particles. Comp Sci Technol 2009;69:1653–1659.
34. Renner K, Kenyó C, Móczó J, Pukánszky B. Micromechanical deformation processes in PP/wood composites: Particle characteristics, adhesion, mechanisms. Compos Part A 2010;41:1653–1661.
35. Clemons C. Elastomer modified polypropylene–polyethylene blends as matrices for wood flour–plastic composite. Compos Part A 2010;41:1559–1569.
36. Oksman K. Improved interaction between wood and synthetic polymers in wood/polymer composites. Wood Sci Technol 1996;30:197–205.
37. Oksman K, Clemons C. Mechanical properties and morphology of impact modified polypropylene–wood flour composites. J Appl Polym Sci 1998;67:1503–1513.
38. Dányádi L, Janecska T, Szabó Z, Nagy G, Móczó J, Pukánszky B. Wood flour filled PP composites: Compatibilization and adhesion. Comp Sci Technol 2007;67:2838–2846.
39. Pukánszky B, Móczó J. Morphology and properties of particulate filled polymers. Macromol Symp 2004;214:115-134.

40. Faludi G, Link Z, Renner K, Móczó J, Pukánszky B. Factors determining the performance of thermoplastic polymer/wood composites; the limiting role of fiber fracture. Mater Design 2014;61:203-210.
41. Nicolais L, Narkis M. Stress-strain behavior of styrene-acrylonitrile/glass bead composites in the glassy region. Polym Eng Sci 1971;11:194-199.

7. CAPTIONS

Fig. 1 Composition dependence of the Young's modulus of PP/MAEPDM/wood composites. Effect of elastomer content and structure. Symbols: ☐ PP, ■ PP/MAPP, ○ PP/5 wt% MAEPDM, ◑ PP/10 wt% MAEPDM, ● PP/20 wt% MAEPDM

Fig. 2 Effect of material combination on the stiffness of multicomponent multiphase PP composites at 10 wt% elastomer content. Symbols: ☐ PP, ■ PP/MAPP, ◭ PP/EPR, ◆ PP/EPR/MAPP, ◑ PP/MAEPDM

Fig. 3 SEM micrograph recorded on the fracture surface of a PP composite containing 30 wt% wood and 20 wt% MAEPDM as separately dispersed wood particles and elastomer droplets.

Fig. 4 Changes in the tensile yield stress of multicomponent PP composites at 10 wt% elastomer content with composition. Effect of adhesion and wood content. Symbols: ☐ PP, ■ PP/MAPP, ◭ PP/EPR, ◆ PP/EPR/MAPP, ◑ PP/MAEPDM

Fig. 5 Acoustic emission testing of a PP/wood composite. Wood content: 30 wt%. ○ individual acoustic events. Stress vs. strain and cumulative No. of signal vs. strain traces.

Fig. 6 Comparison of the stress vs. strain and cumulative No. of signal traces for the five material combinations studied. Wood content: 30 wt%, elastomer content: 10 wt%. Notation: ———— PP, - - - - PP/MAPP, - · - · - · PP/EPR, ---- PP/EPR/MAPP, ····· PP/MAEPDM

Fig. 7 Effect of composition on the characteristic stress (σ_{AE2}) of the dominating local deformation process in PP/MAEPDM/wood composites. Symbols: ☐ PP, ■ PP/MAPP, ○ PP/5 wt% MAEPDM, ◑ PP/10 wt% MEPDM, ● PP/20 wt% MAEPDM.

Fig. 8 Dependence of average stresses developing in the matrix and initiating local deformations around the particles on wood content. Initiation stresses corrected for zero load bearing of the MAEPDM elastomer (σ_{AE}^{corr}). Symbols are the same as in Fig. 7.

Fig. 9 Corrected characteristic stresses plotted against wood content for the five material combinations studied. Elastomer content: 10 wt%. Symbols: ☐ PP, ■ PP/MAPP, △ PP/EPR, ◇ PP/EPR/MAPP, ○ PP/MAEPDM. Empty symbols indicate the first (σ_{AE1}), while the rest the second acoustic emission process (σ_{AE2}).

Fig. 10 Local deformation processes occurring in the various material combinations at 30 wt% wood content; a) fiber fracture, PP/MAPP, b) debonding, PP/20 wt% EPR, c) debonding and pull-out PP/20 wt% EPR, d) wood fracture, PP/MAPP/20 wt% EPR.

Fig. 11 Effect of processing conditions on the dispersed structure of multicomponent PP composites. Empty symbols: MAPP, good adhesion, separate dispersion; full symbols: MAEPDM, limited embedding; (○,●) injection molding, (☐,■) internal mixer.

Fig. 12 Dependence of composite strength on the initiation stress of the dominating local deformation process. Empty symbols indicate 5 wt%, half-empty symbols 10 wt% and filled symbols 20 wt% elastomer content. Symbols: ☐ PP, ■ PP/MAPP, △ PP/EPR, ◇ PP/EPR/MAPP, ○ PP/MAEPDM.

Sudár, Fig. 1

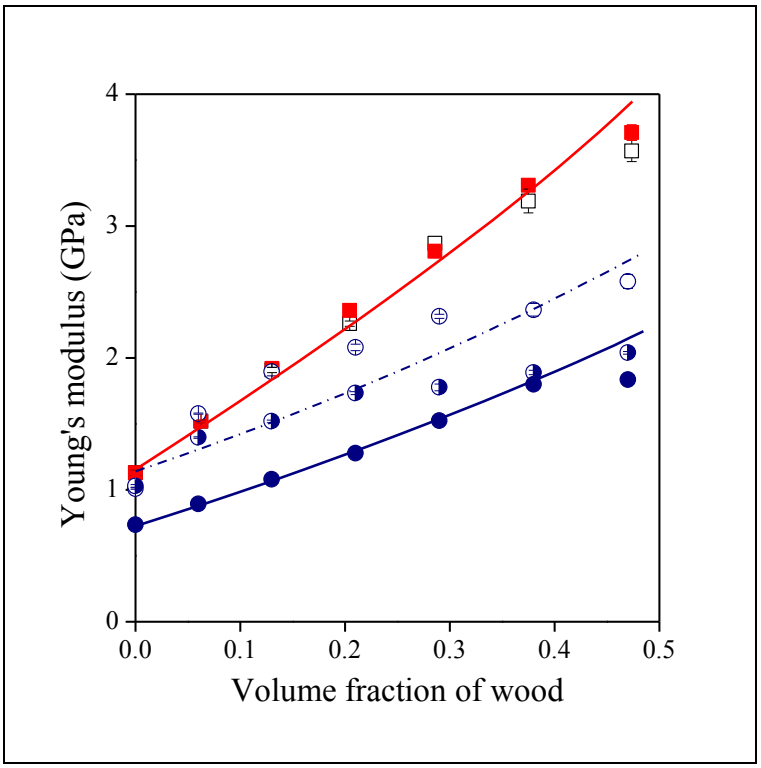

Sudár, Fig. 2

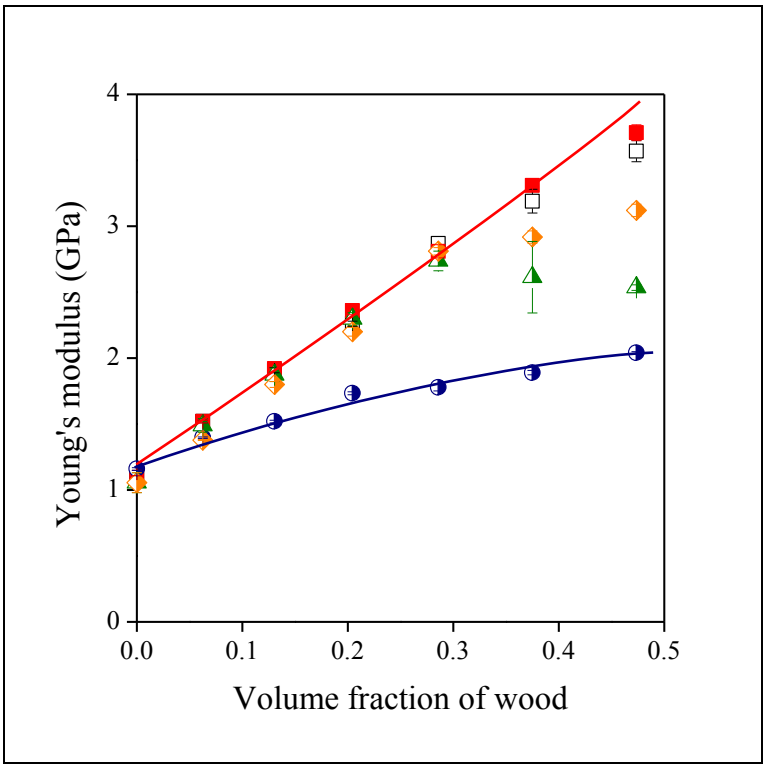

Sudár, Fig. 3

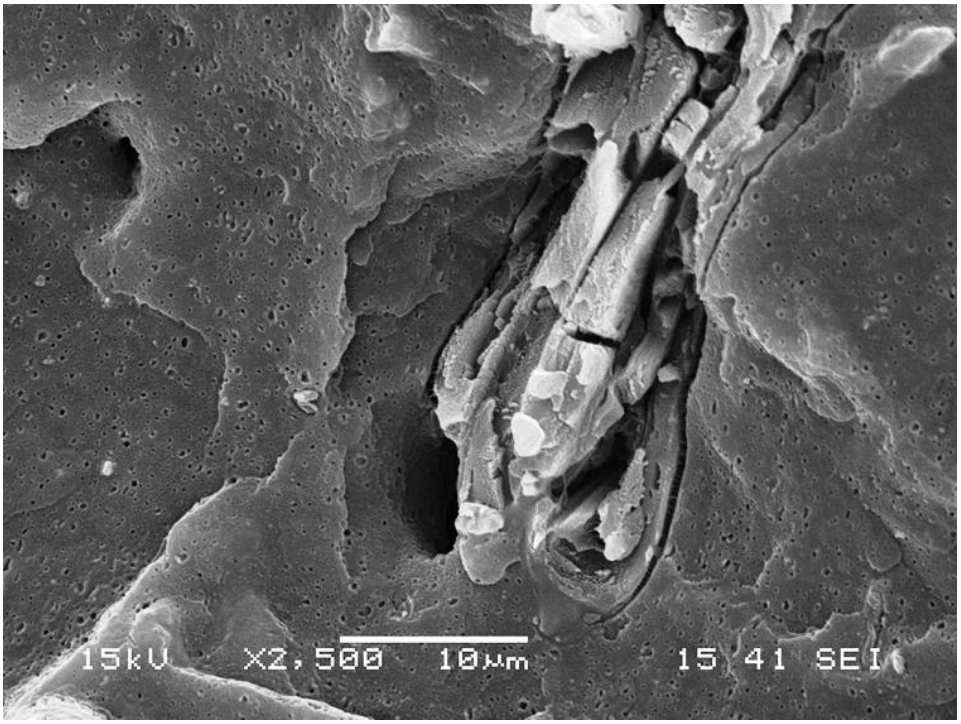

Sudár, Fig. 4

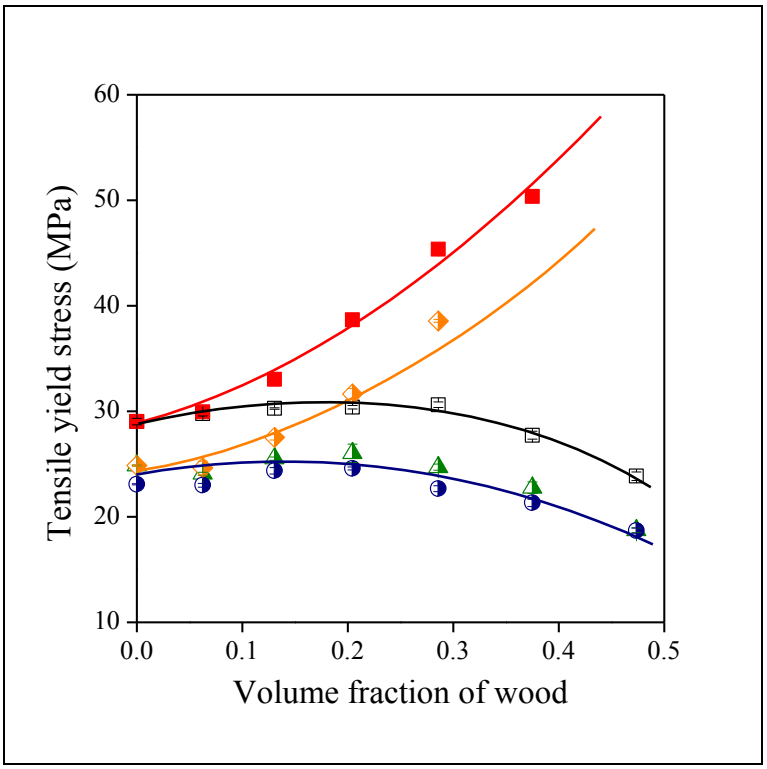

Sudár, Fig. 5

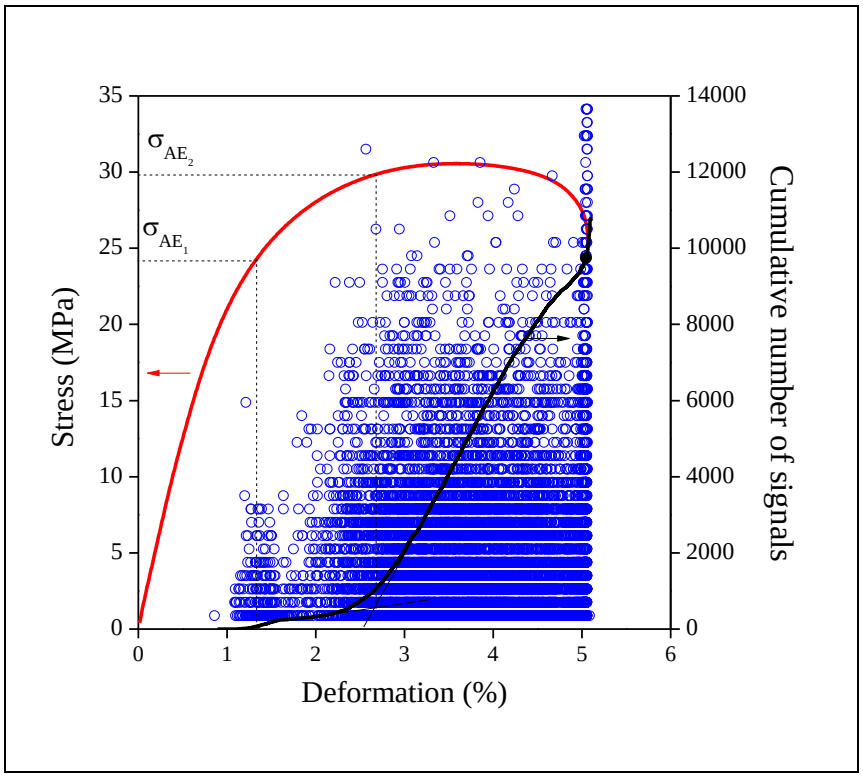

Sudár, Fig. 6

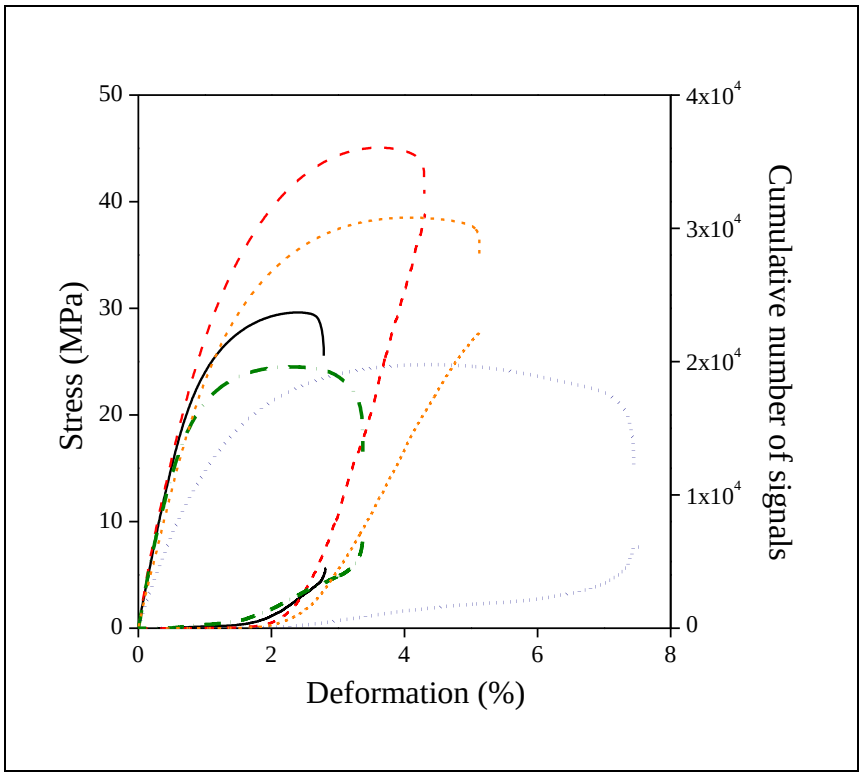

Sudár, Fig. 7

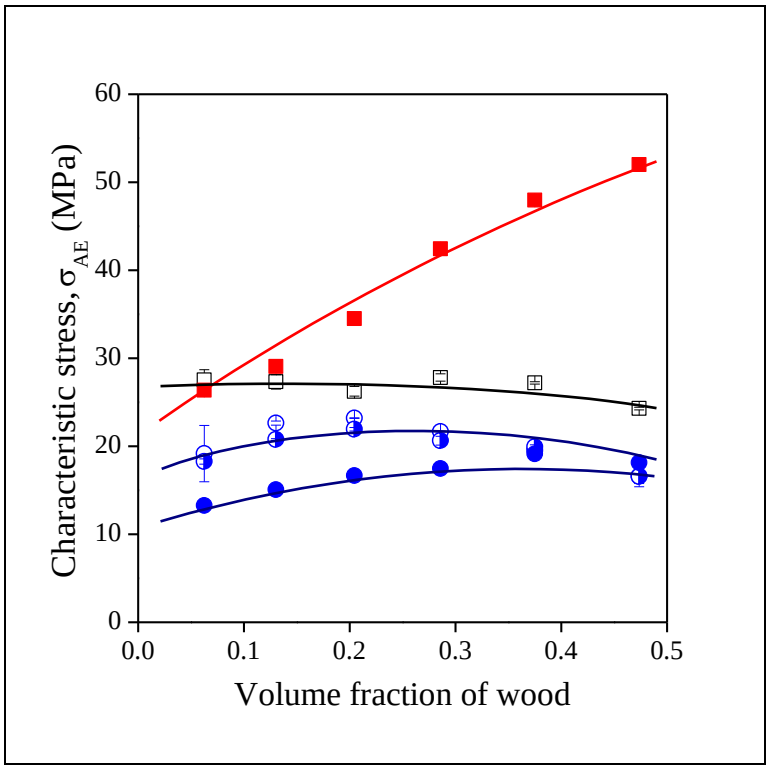

Sudár Fig. 8

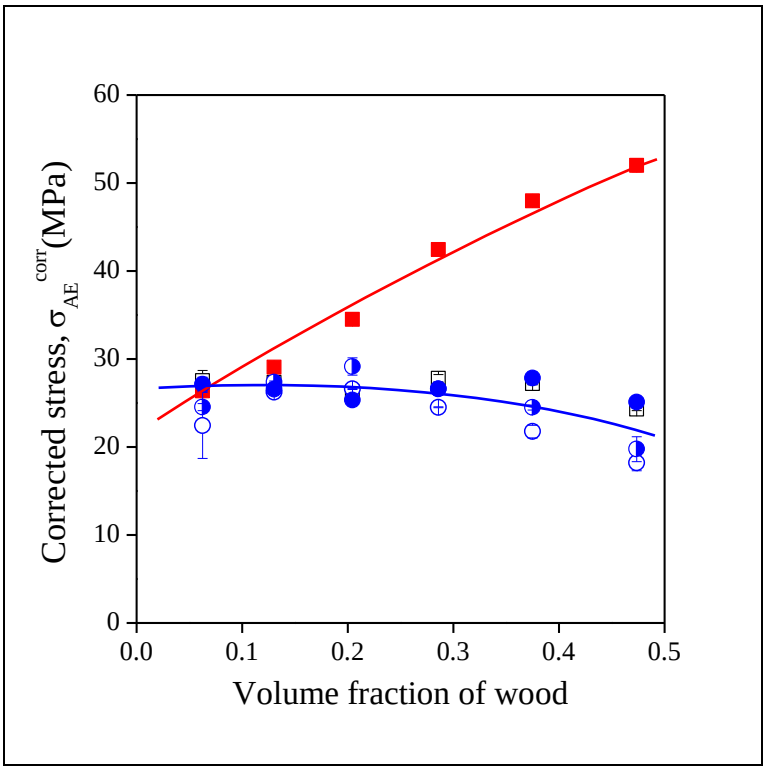

Sudár, Fig. 9

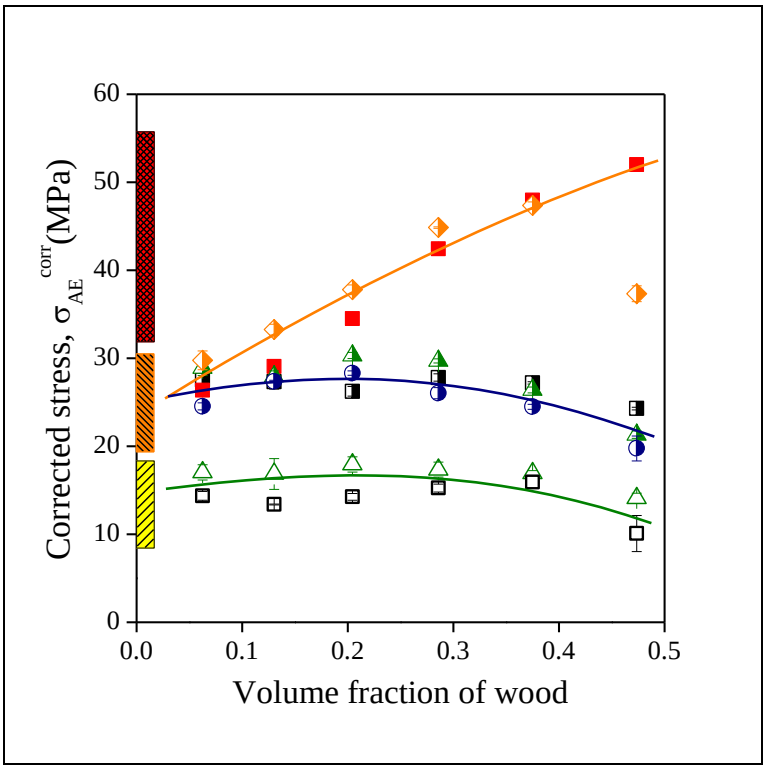

Sudár, Fig. 10

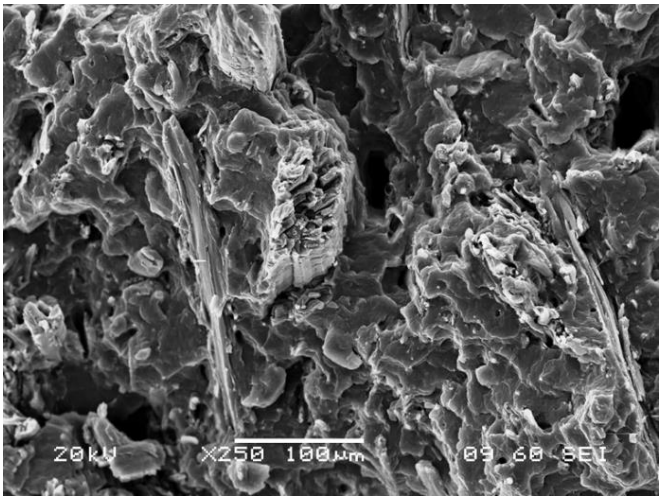

a)

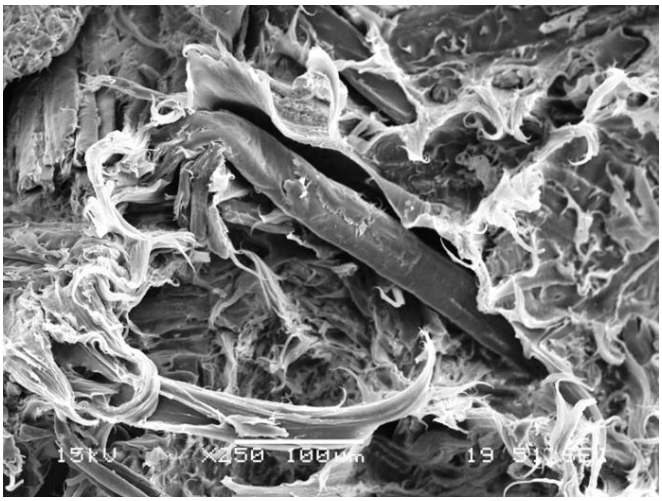
15kV
X250 100µm

b)

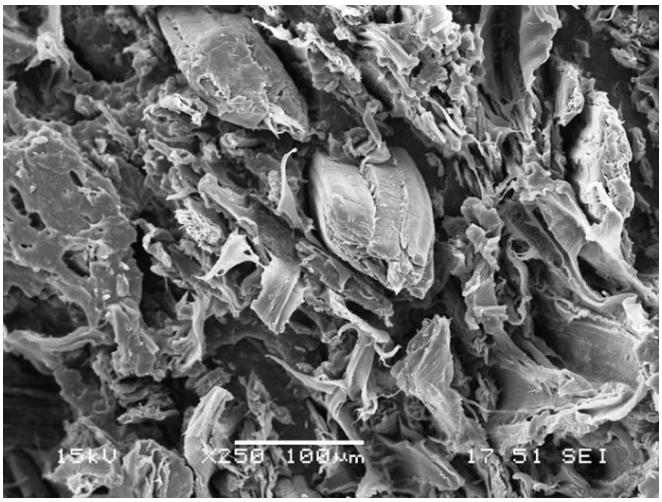
15kV
X250 100µm
17 51 SEI

c)

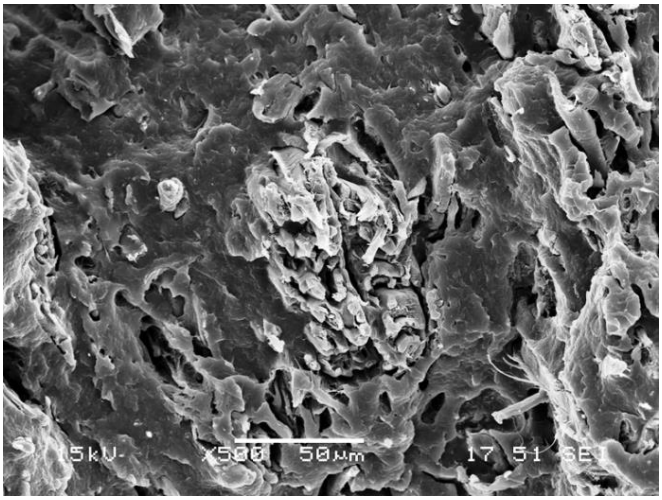
15kV
X500 50µm
17 51 SE

d)

Sudár, Fig. 11

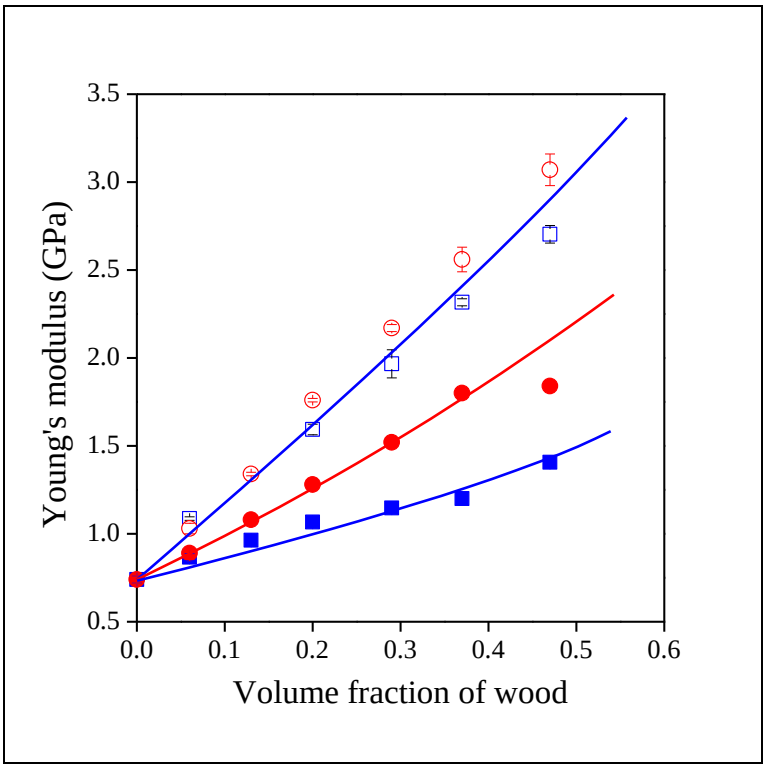

Sudár, Fig. 12